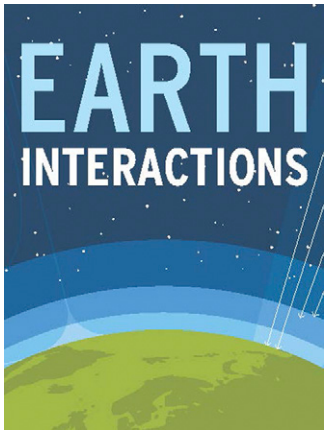

Copyright © 2015, Paper 19-016; 41347 words, 10 Figures, 0 Animations, 6 Tables.
http://EarthInteractions.org

Reduction of Global Plant Production due to Droughts from 2001 to 2010: An Analysis with a Process-Based Global Terrestrial Ecosystem Model

Chang Liao and Qianlai Zhuang*

Department of Earth, Atmospheric, and Planetary Sciences, Purdue University, West Lafayette, Indiana

Received 21 July 2014; in final form 15 September 2015

ABSTRACT: Droughts dramatically affect plant production of global terrestrial ecosystems. To date, quantification of this impact remains a challenge because of the complex plant physiological and biochemical processes associated with drought. Here, this study incorporates a drought index into an existing process-based terrestrial ecosystem model to estimate the drought impact on global plant production for the period 2001–10. Global Moderate Resolution Imaging Spectroradiometer (MODIS) gross primary production (GPP) data products are used to constrain model parameters and verify the

* Corresponding author address: Qianlai Zhuang, Department of Earth, Atmospheric, and Planetary Sciences, Purdue University, 550 Stadium Mall Drive, West Lafayette, IN 47907-2051.
E-mail address: qzhuang@purdue.edu

DOI: 10.1175/EI-D-14-0030.1

model algorithms. The verified model is then applied to evaluate the drought impact. The study indicates that droughts will reduce GPP by 9.8 g C m^{-2} $month^{-1}$ during the study period. On average, drought reduces GPP by 10% globally. As a result, the global GPP decreased from 106.4 to 95.9 Pg C yr^{-1} while the global net primary production (NPP) decreased from 54.9 to 49.9 Pg C yr^{-1}. This study revises the estimation of the global NPP and suggests that the future quantification of the global carbon budget of terrestrial ecosystems should take the drought impact into account.

KEYWORDS: Drought; Extreme events; Ecological models

1. Introduction

Drought is recognized as one of the most damaging natural disasters worldwide, which severely impacts the ecosystem goods and services. The fifth assessment report of Intergovernmental Panel on Climate Change (IPCC) stated that confidence is low for a global-scale observed trend in drought or dryness (lack of rainfall) and the frequency and intensity of drought have likely increased during the last century (IPCC 2013). In general, drought is defined as a period of abnormally dry weather long enough to cause a serious hydrological imbalance (Planton 2013). Droughts usually negatively impact the terrestrial ecosystems. For instance, droughts, especially extreme droughts, reduce the ecosystem productivity (Ciais et al. 2005; Zhao and Running 2010). Therefore, droughts could substantially affect the regional and global ecosystem carbon cycling (Chen et al. 2012; Rajan et al. 2013).

To assess drought severity, drought indices including the Palmer drought severity index (PDSI), standardized precipitation index (SPI)/standardized precipitation evapotranspiration index (SPEI), and drought severity index (DSI) have been developed (McKee et al. 1993; Mu et al. 2013; Palmer 1965; Vicente-Serrano et al. 2010). PDSI and its variations (e.g., self-calibrated PDSI) are widely used for meteorological drought monitoring and assessment, especially in the United States (Palmer 1965; Wells et al. 2004). The response of global biome to drought was examined using SPEI (Vicente-Serrano et al. 2013). Furthermore, SPI has been used to analyze the drought impacts on carbon dynamics (Shi et al. 2013). For decades, drought indices merely serve as end products for drought monitoring and assessment, yet seldom have they been used in ecosystem modeling. Most studies focused on analyzing the correlations between drought indices and other variables such as gross primary production (GPP) and normalized difference vegetation index (NDVI). Those studies generally imply a causative relation between droughts and ecosystem productivity (Shi et al. 2013; Vicente-Serrano et al. 2015). Meanwhile, vegetation indices including leaf area index (LAI) and NDVI are intensively used in ecosystem modeling (Hashimoto et al. 2012; Huete et al. 2002; Rossini et al. 2012). However, no studies have attempted to incorporate drought indices into ecosystem modeling at the global scale.

Ideally, a number of drought impact mechanisms instead of drought indexes should be incorporated into ecosystem modeling. First, different organs (e.g., leaves and roots) of plants respond to droughts at different time scales. For example, leaf stomatal closure responds to droughts instantly, while the root system response may take months or longer. Drought-induced gene changes could take years or generations (Chaves et al. 2003; Reyer et al. 2013). Second, plants respond

to water deficits through a series of physiological and biochemical processes at different ecosystem levels (Chaves et al. 2003; Reddy et al. 2004). At a leaf level, the photosynthesis process is constrained through stomatal closure to reduce water loss (Reddy et al. 2004). At the same time, plants tend to maintain high tissue water potential to avoid tissue dehydration. Some plants also tend to shorten their growth cycles or complete life cycles before physiological water deficits occur (Eilmann et al. 2011; Vicente-Serrano et al. 2013). Under severe or extreme drought conditions, most plant activities, including photosynthesis, are impaired, potentially causing plant mortality (McDowell et al. 2008; Sala et al. 2010; Sitch et al. 2008). To date, ecosystem modeling indeed has made good progress in accounting for drought effects on photosynthesis by considering the effects of drought stress on stomatal closure, vapor pressure deficit, and other controls (Sitch et al. 2003, 2008). However, these ecosystem models did not explicitly consider the drought severity, especially the extreme droughts. These models also did not distinguish the differences in responses from one plant function type (PFT) to another.

It is also important to incorporate the time-lag effects into ecosystem modeling. This is because different PFTs respond to drought stress at different time scales (Welp et al. 2007; Chaves et al. 2003; Sitch et al. 2008). A few studies have shown that the time lag can range from an instantaneous response to several months or even decades for large trees (Barber et al. 2000; Sitch et al. 2008). Globally, most plants respond predominantly to drought with a short time lag of 2 to 4 months (Vicente-Serrano et al. 2013).

It is also a challenge to quantify drought impacts at the global scale because plants in different regions have different responses. For instance, in arid regions, plants are more resistant to drought. This might be attributed to their adaption to water deficits through physiological, anatomical, and functional strategies. However, their time lag is normally shorter (<6 months) compared to that of plants in humid ecoregions (Vicente-Serrano et al. 2012, 2013). Vegetation in humid regions, such as tropic and subtropic ecoregions, could be sensitive to drought as water shortage rarely occurs (Engelbrecht et al. 2007; Phillips et al. 2009). Meanwhile, vegetation in semiarid and semihumid ecoregions tends to have a longer time lag. In these regions, plants can tolerate mild droughts but would be negatively affected if drought persisted (Vicente-Serrano et al. 2013). Most vegetation in subarid ecoregions has the longest time lag (Vicente-Serrano et al. 2013). But the time lag in these ecoregions might be less than 6 months for the growing season (Rouault and Richard 2003). In subhumid ecoregions, where water balance approaches zero, the time lag is usually between 8 and 10 months (Vicente-Serrano et al. 2013); the time lag decreases as water availability increases to less than 5 months (Vicente-Serrano et al. 2013). For grasslands, the maximum correlation between NDVI and water deficits is found to be around 1 month during the growing season, which means the time lag might be 1 month (Wang et al. 2001). For woodlands, the time lag is approximately 2 months in summer. The time lag for agricultural ecosystems is from 3 to 6 months (Rouault and Richard 2003). In summary, different PFTs have different time lags in response to droughts. However, despite the rich knowledge of time-lag effects, current ecosystem models have not explicitly considered these effects.

Here, we make the first attempt to incorporate the drought index into ecosystem modeling to estimate the drought impact on ecosystem carbon cycling considering

both the drought severity and time-lag effects. The MODIS GPP data are used for model parameterization and verification. Specifically, we incorporate PDSI into a process-based biogeochemistry model, the Terrestrial Ecosystem Model (TEM) (Zhuang et al. 2003, 2010), to assess the drought impact on plant primary production at the global scale from 2001 to 2010.

2. Method

2.1. Overview

We use a model data assimilation approach to improve the ecosystem model capability of estimating the drought impact on plant productivity (Figure 1). The Terrestrial Ecosystem Model (Zhuang et al. 2003, 2010) is used. We develop an empirical function to account for drought impacts on GPP using MODIS GPP data products and drought data in the period of 2001–10. The empirical relationship is then incorporated into TEM. A portion of MODIS GPP data is used to parameterize the revised TEM. The remaining MODIS GPP data are used to verify the revised TEM. Finally, we extrapolate the model to quantify the global plant primary production considering the drought impact.

2.2. Modification of the Terrestrial Ecosystem Model

The Terrestrial Ecosystem Model is a process-based ecosystem model driven with air temperature, precipitation, and radiation to estimate terrestrial ecosystem carbon and nitrogen dynamics (Zhuang et al. 2003, 2010). In TEM, GPP is carbon assimilation by plants through photosynthesis. Net primary production (NPP) is the total amount of carbon stored by plants, which considers both the photosynthesis and maintenance respiration. GPP is modeled as a function of atmospheric CO_2 concentration, photosynthetically active radiation (PAR), air temperature, nitrogen availability, and other variables:

$$\begin{aligned} \mathrm{GPP} = {} & C_{\max} f(\mathrm{CO_2}) f(\mathrm{PAR}) f(\mathrm{Phenology}) f(\mathrm{Foliage}) \\ & f(T) f(C_A, C_v) f(\mathrm{NA}) f(\mathrm{FT}), \end{aligned} \tag{1}$$

where $C_{\max}$ is the maximum rate of carbon assimilation by the entire plant canopy under optimal environmental condition; $f(\mathrm{CO_2})$ represents CO_2 concentration limitation; $f(\mathrm{PAR})$ represents the photosynthetically active radiation limitation; $f(\mathrm{Phenology})$ represents the leaf area limitation; $f(\mathrm{Foliage})$ is the ratio of canopy leaf biomass relative to maximum leaf biomass; and $f(C_A, C_v)$ represents the control of leaf internal CO_2 concentration change resulting from water deficits. NPP is the difference between plant respiration and GPP:

$$\mathrm{NPP} = \mathrm{GPP} - R_A, \tag{2}$$

where R_A is the plant respiration, which is estimated as a function of plant biomass and air temperature using the classical Q_{10} function. A more detailed description of the model can be found in Zhuang et al. (2003) and Chen et al. (2011).

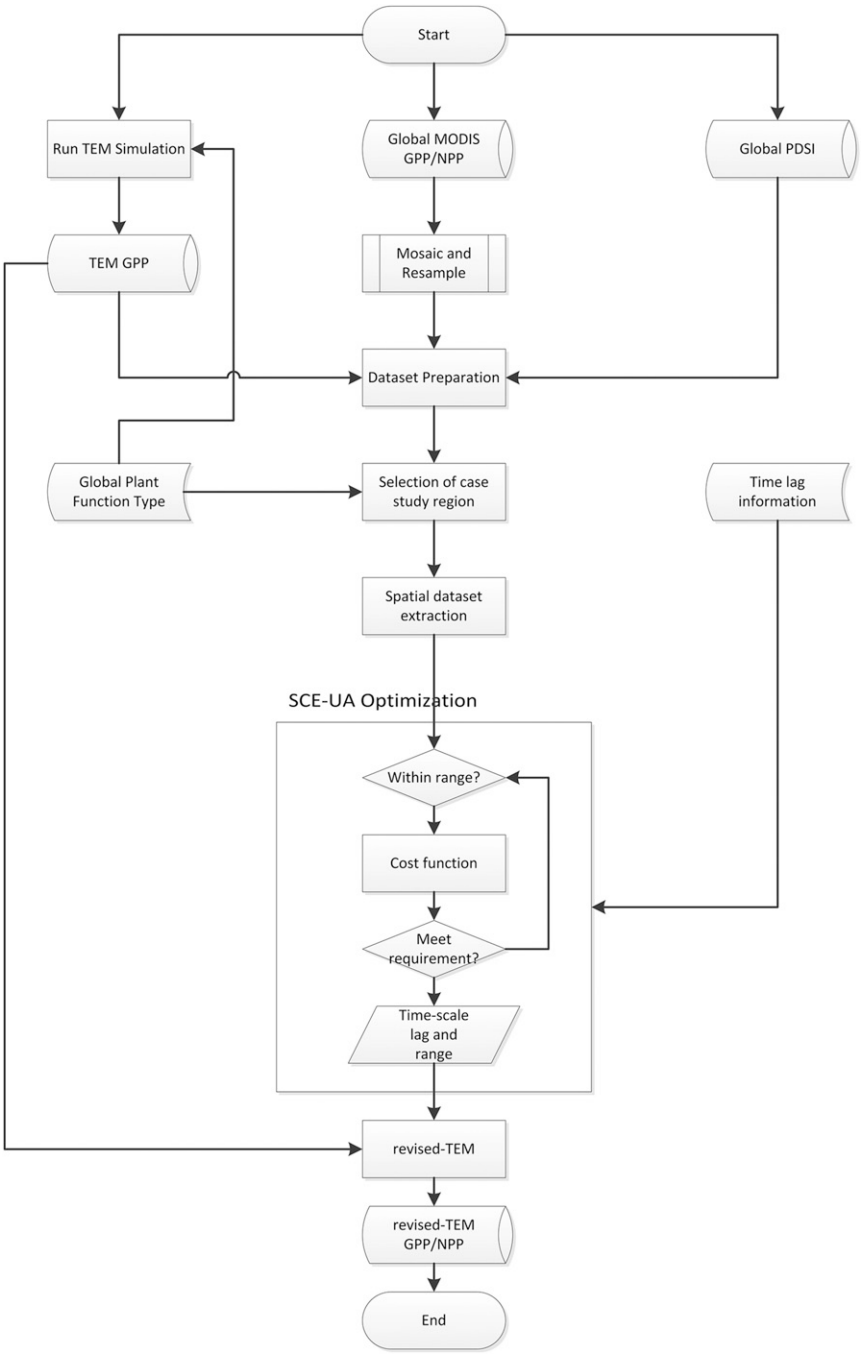

Figure 1. Flowchart of modeling analysis of drought effects on plant production.

In TEM, both GPP and R_A are directly influenced by droughts. For instance, CO_2 diffusion to leaves is affected by the evapotranspiration (ET) rate, which is determined by soil water deficits and stomatal closure, both affected by drought conditions. To some extent, TEM models' mild drought impacts GPP. However, similar to other

Table 1. Drought conditions indicated with PDSI.

Category	PDSI range	Drought condition
W5	4.0 or greater	Extreme wet
W4	3.0 to 3.99	Very wet
W3	2.0 to 2.99	Moderate wet
W2	1.0 to 1.99	Slightly wet
W1	0.5 to 0.99	Incipient wet
WD	−0.49 to 0.49	Normal
D1	−0.50 to −0.99	Incipient drought
D2	−1.00 to −1.99	Mild drought
D3	−2.00 to −2.99	Moderate drought
D4	−3.00 to −3.99	Severe drought
D5	−4.00 or less	Extreme drought

ecosystem models, its current algorithms are not able to account for various levels of droughts and time-lag effects on plant productivity.

Here, we incorporate a drought index PDSI, which provides comprehensive information of drought stress into the TEM model to account for drought effects on carbon cycling. PDSI is a widely used drought index (Alley 1984; Dai 2011; Palmer 1965).

The general classification of the drought severity condition based on the PDSI is listed in Table 1. PDSI and its variations have been extensively used for drought monitoring and assessment regardless their limitations and assumptions (Alley 1984; Guttman 1998). In this study, the PDSI factor is added to the GPP estimation:

$$\begin{aligned} \mathrm{GPP}_{\mathrm{Revised}} = C_{\max} f(\mathrm{CO_2}) f(\mathrm{PAR}) f(\mathrm{Phenology}) f(\mathrm{Foliage}) \\ f(T) f(C_A, C_v) f(\mathrm{NA}) f(\mathrm{FT}) f(\mathrm{PDSI}), \end{aligned} \tag{3}$$

where $f(\mathrm{PDSI})$ represents the effects of drought, which is defined as

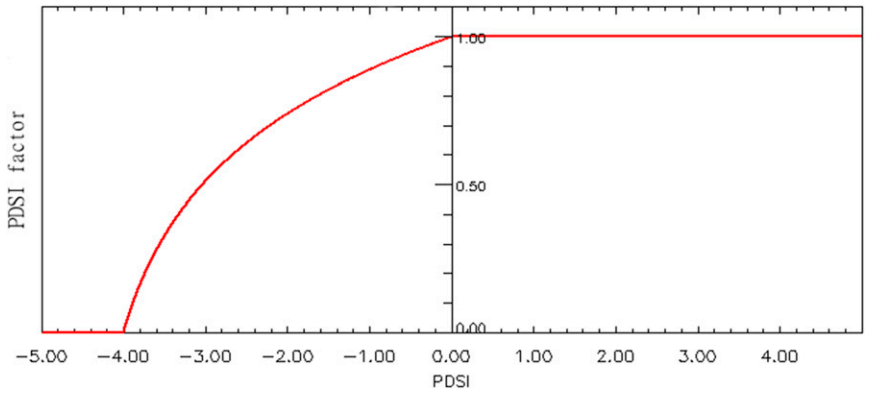

Figure 2. PDSI model piecewise function illustration. The *x* axis is the PDSI, in which the more negative the value, the more severe the drought condition. The *y* axis is the PDSI factor calculated using Equation (4). The factor ranges between 0.0 and 1.0 and intersect with *x* axis at threshold A, reaching 1.0 at threshold B.

Table 2. The time lags (months) for different plant function types.

Plant function type	Time lag	References
The alpine tundra and the polar desert	1–12	(Brock and Galen 2005; Vicente-Serrano et al. 2013)
Wet tundra	3–9	(Vicente-Serrano et al. 2013)
Boreal forest	6–12	(Peng et al. 2011; Vicente-Serrano et al. 2013; Welp et al. 2007)
Temperate coniferous forests	8–10	(Lévesque et al. 2013; Vicente-Serrano et al. 2013)
Temperate deciduous forests	1–8	(Vicente-Serrano et al. 2013)
Grasslands	1–6	(Craine et al. 2012; Vicente-Serrano et al. 2013)
Xeric shrub lands	4–7	(Vicente-Serrano et al. 2013)
Tropical forests	1–12	(Engelbrecht et al. 2007; Kumagai and Porporato 2012; Vicente-Serrano et al. 2013)
Xeric woodlands	2–6	(Vicente-Serrano et al. 2013)
Temperate evergreen broadleaf	1–12	(Vicente-Serrano et al. 2013)

$$f(\mathrm{PDSI})_m = \begin{cases} 0.0 & \text{when} \quad \mathrm{PDSI}_{m-l} < A \\ \log(X\,\mathrm{PDSI}_{m-l} + Y) & \text{when} \quad A \le P\mathrm{DSI}_{m-l} \le B \\ 1.0 & \text{when} \quad \mathrm{PDSI}_{m-l} > B \end{cases}, \tag{4}$$

where $f(\mathrm{PDSI})_m$ is the PDSI factor for the mth month; PDSI_{m-l} is the PDSI value with a time lag of l months; A and B are the lower and upper thresholds parameters; and X and Y are the shape parameters of the logarithm curve.

When PDSI_{m-l} is lower than the threshold A, which indicates the extreme drought, $f(\mathrm{PDSI})_m = 0.0$. On the contrary, when PDSI_{m-l} is greater than the

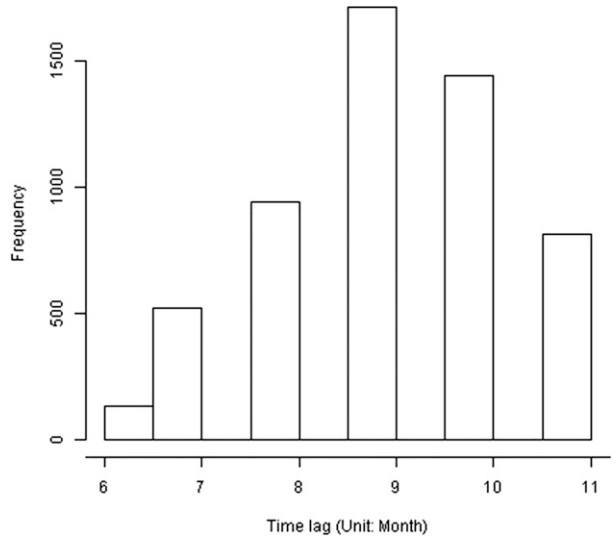

Figure 3. Histogram of time lags for temperate coniferous forests. The *x* axis is the time lag (month). The *y* axis is the frequency.

Table 3. Global optimization results of time lag (months) and thresholds for PDSI model using SCE-UA method and histogram method for 10 plant function types.

Plant function type	Time-scale lag	Threshold A	Threshold B
The alpine tundra and polar desert	8	−5.50	−1.00
Wet tundra	9	−5.5	−1.00
Boreal forest	9	−5.5	−1.00
Temperate coniferous forests	10	−4.5	−1.75
Temperate deciduous forests	8	−4.0	0.0
Grasslands	6	−4.0	−1.75
Xeric shrub lands	7	−5.5	−1.75
Tropical forests	6	−4.0	−1.75
Xeric woodlands	6	−5.5	−1.75
Temperate evergreen broadleaf	6	−5.5	0.0

threshold B, which means no drought or incipient drought, or even wet condition, the drought impact is negligible; therefore, $f(\text{PDSI})_m = 1.0$. When PDSI_{m-l} lies between the lower and upper bounds, the logarithm curve is used to model drought effects based on a power-law impact distribution (Reichstein et al. 2013; Zscheischler et al. 2014). An ideal case of this piecewise-defined function is illustrated in Figure 2 (when threshold $A = -4.0$ and threshold B = 0.0 from Table 1). All parameters vary with PFTs.

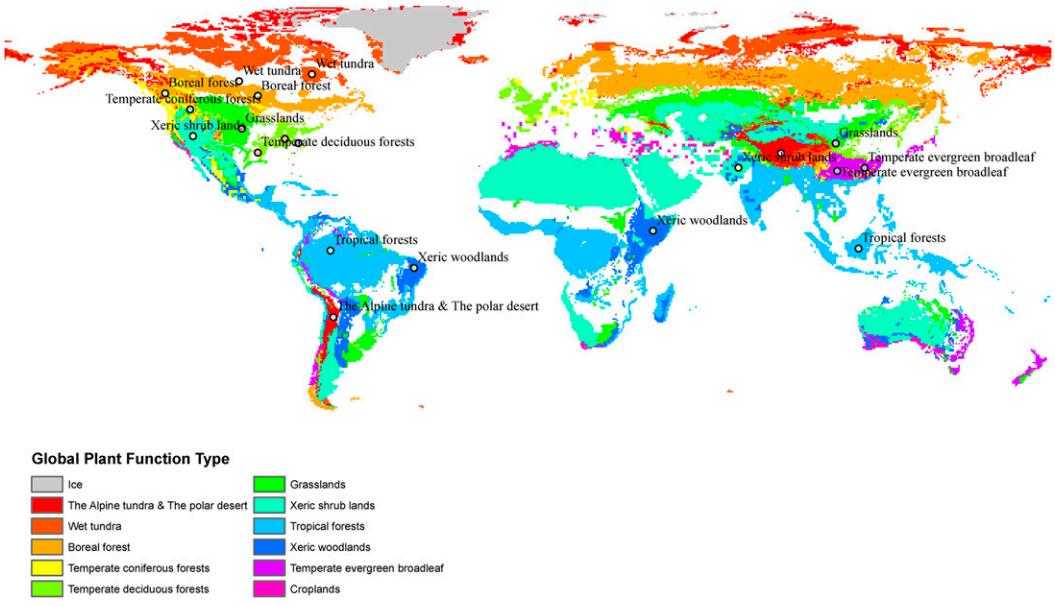

Figure 4. Global plant function–type distribution and case study regions. The points are the spatial locations of case study regions for 10 plant function types, from which cropland is excluded. For each plant function type, two case study regions are selected for model verification.

Table 4. Spatial–temporal attributes of the spatial datasets used in this study.

	PDSI	MODIS GPP	MODIS NPP	TEM GPP
Data source	NCAR CGD's Climate Analysis Section	MODIS Land MOD17A2	MODIS Land MOD17A3	TEM simulation
Spatial resolution	2.5° × 2.5°	Global 1 km × 1 km	Global 1 km × 1 km	0.5° × 0.5°
Temporal resolution	Monthly	8 days	Annual	Monthly

2.3. Model parameterization and global simulations

To estimate the parameters in Equation (4), we employed the shuffled complex evolution (SCE-UA) parameter optimization method, which has been widely used in hydrologic model parameter optimization (Duan et al. 1994). The SCE-UA method requires initial parameter values, lower and upper boundaries of the parameters, and a cost function. The boundary condition and initial values of time lag and thresholds were determined based on literature (Table 2). The cost function was from (Tarantola 2005; Thiemann et al. 2001)

$$S = [g(m) - d_{\text{obs}}]^t C_d^{-1} [g(m) - d_{\text{obs}}], \tag{5}$$

where $g(m)$ is the theoretical prediction, d_{obs} is the observation, and C_d is the covariance matrix.

The global parameter optimization method (SCE-UA) was applied for each plant function type to estimate the time lag and thresholds parameters. For example, for the temperate coniferous forest, SCE-UA was conducted over all pixels for a region. The most frequent time lag, 9 months, was determined from the optimization results based on the histogram (Figure 3). Further examinations have shown that our parameterization results are consistent with literature (Tables 2 and 3).

We first apply the model to case study regions to obtain parameters for the empirical function for various PFTs (Figure 4). We then extrapolate the model and parameters globally. The simulated plant production with two versions of TEM and MODIS data are compared.

2.4. Data

The global PDSI data are obtained from the National Center for Atmospheric Research (NCAR) Climate and Global Dynamics (CGD) Climate Analysis Section (http://www.cgd.ucar.edu/cas/catalog/climind/pdsi.html) at a monthly time step and 2.5° × 2.5° spatial resolution. TEM GPP is simulated at a monthly time step and 0.5° × 0.5° spatial resolution at the global scale from 2001 to 2010 (Table 4). The auxiliary global PFT distribution data are obtained from previous studies (Zhuang et al. 2003).

The MODIS GPP data are obtained from NASA Land Processes Data Active Archive Center (LP DAAC). The spatial–temporal resolution is 8 day and 1 km ×

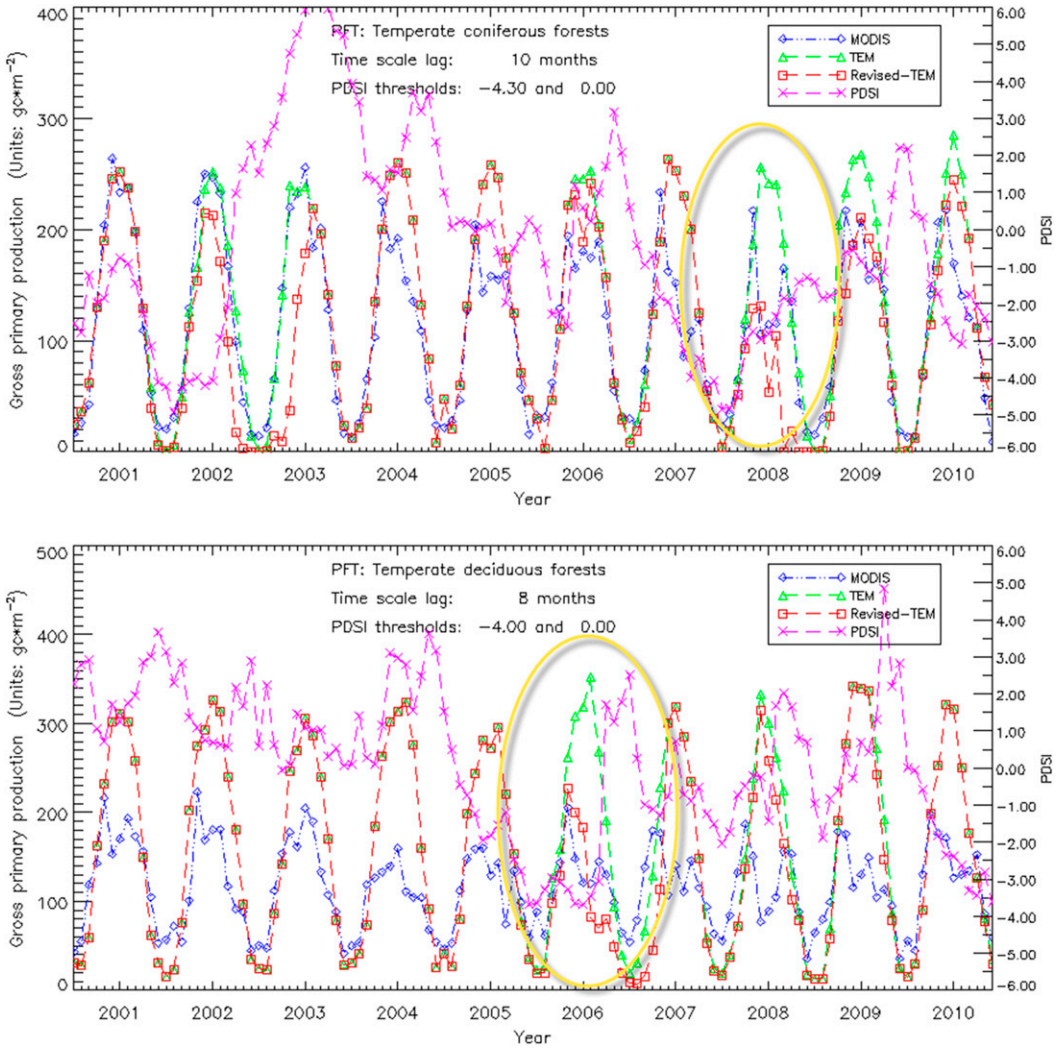

Figure 5. Comparison between MODIS GPP, TEM GPP, and revised TEM GPP for temperate coniferous forests and temperate deciduous forests during 2001–10. Since the time lag is 10/8 months, the TEM GPP and revised TEM GPP are identical for the first 10/8 months. The *x* axis is the time from year 2001 to 2010. The left *y* axis is the GPP estimation ($g\,m^{-2}$). The right *y* axis is the PDSI (dimensionless). The line connecting diamonds is the MODSI GPP estimation, the line connecting triangle is the TEM GPP estimation, and the line connecting square is the revised TEM GPP estimation and the line connecting cross is the PDSI trend.

1 km. The MODIS NPP datasets are obtained from NASA LP DAAC at an annual time step and 1 km × 1 km spatial resolution.

The MODIS GPP is estimated using the light use efficiency (LUE) approach. The daily GPP is estimated as below:

Table 5. RMSE comparisons between TEM GPP and revised TEM GPP for case study regions (g C m^{-2} $month^{-1}$).

Plant function type	TEM	Revised TEM
The alpine tundra and polar desert	7.1	7.1
Wet tundra	0.5	0.5
Boreal forest	19.9	17.4
Temperate coniferous forests	44.2	44.5
Temperate deciduous forests	65.5	45.7
Grasslands	29.1	25.1
Xeric shrub lands	5.4	5.5
Tropical forests	45.4	46.3
Xeric woodlands	36.3	34.8
Temperate evergreen broadleaf	198.9	127.4

$$\mathrm{GPP} = \varepsilon\,\mathrm{APAR}, \tag{6}$$

$$\varepsilon = \varepsilon_{\max}\,\mathrm{TMIN}_{\mathrm{scalar}}\,\mathrm{VPD}_{\mathrm{scalar}}, \tag{7}$$

where ε is the radiation use efficiency; APAR is the absorbed photosynthetically active radiation; $\varepsilon_{\max}$ is the maximum radiation use efficiency; $\mathrm{TMIN}_{\mathrm{scalar}}$ is the air temperature control; and $\mathrm{VPD}_{\mathrm{scalar}}$ is the vapor pressure deficits control (Heinsch et al. 2003). In MODIS GPP algorithms, ε is estimated using the biome parameter lookup table (BPLUT) (Zhao and Running 2010). MODIS GPP data have been verified and widely used in the ecosystem modeling scientific community.

The MODIS GPP data for different ecoregions are selected for model parameterization. (Table 2; Figure 4). Two case study regions are selected for parameterization and verification for each PFT, respectively (Figure 4). The ecoregions experienced recent droughts are chosen, such as the Amazon forest (Phillips et al. 2009) and southern China (NOAA National Centers for Environmental Information 2010).

3. Results and discussion

3.1. Model evaluation

Comparisons between MODIS GPP and two versions of TEM estimations show that TEM generally overestimates GPP, especially when severe drought occurs (Figure 5). The revised TEM constrains the GPP estimation under drought conditions. For instance, when severe drought or extreme droughts occurred in spring of 2008 and summer of 2005 for temperate coniferous forests and temperate deciduous forests, respectively, the revised TEM better estimated GPP (Figures 5a,b). The average RMSE between the revised TEM and MODIS GPP under drought condition for 10 PFTs in case study regions decreased from 45.3 to 35.5 g C m^{-2}. However, the RMSE reduction varies in the case study regions (Table 5).

Spatially, the revised TEM significantly improves the GPP estimation for temperate regions. On average, the RMSE is reduced by 33%. For tropic and Arctic regions, the improvements are moderate. For instance, for alpine tundra

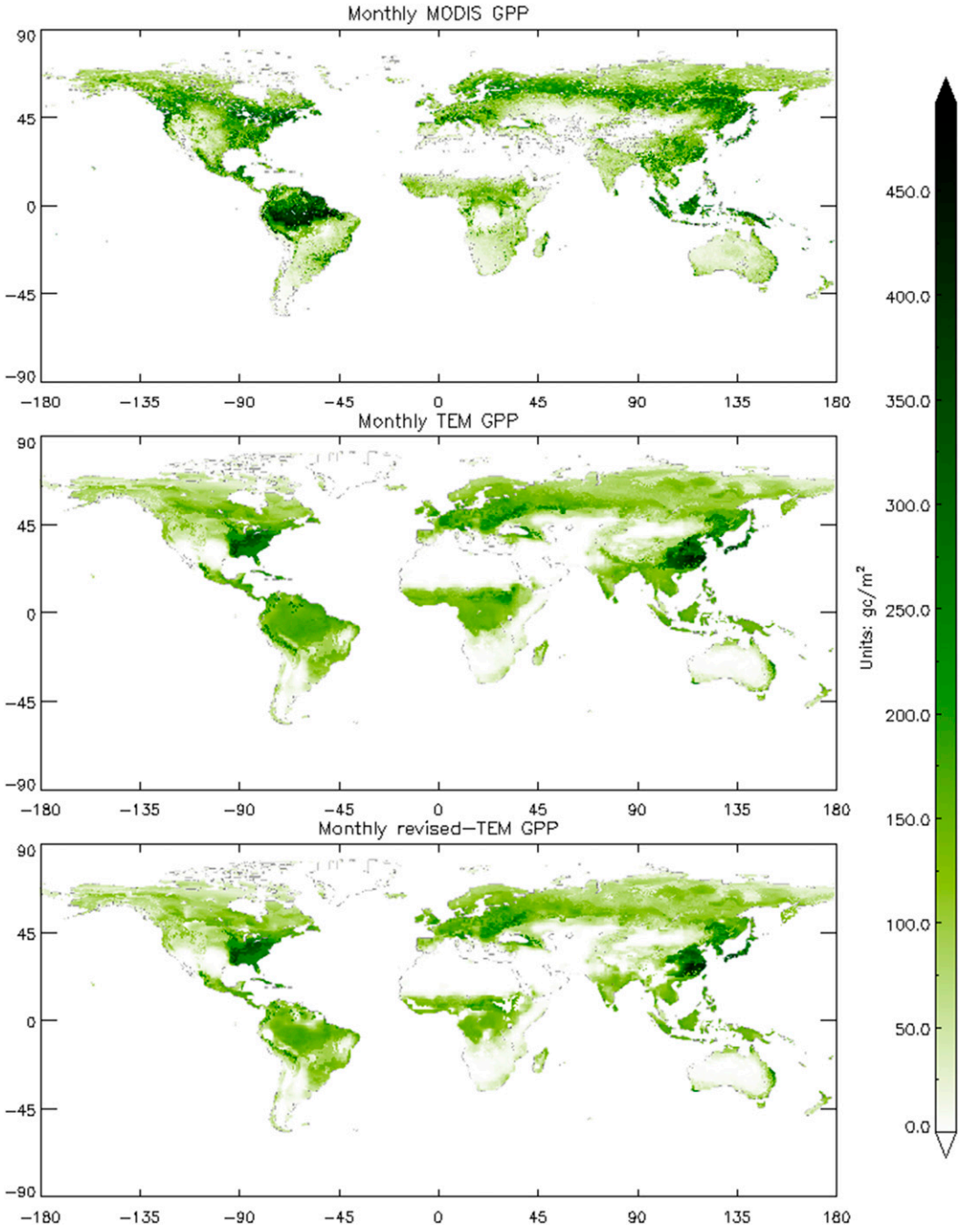

Figure 6. Monthly GPP estimation comparison between MODIS GPP, TEM GPP, and revised TEM GPP for August 2010. Most of the difference between the TEM GPP and revised TEM GPP appears in tropic and temperate ecoregions.

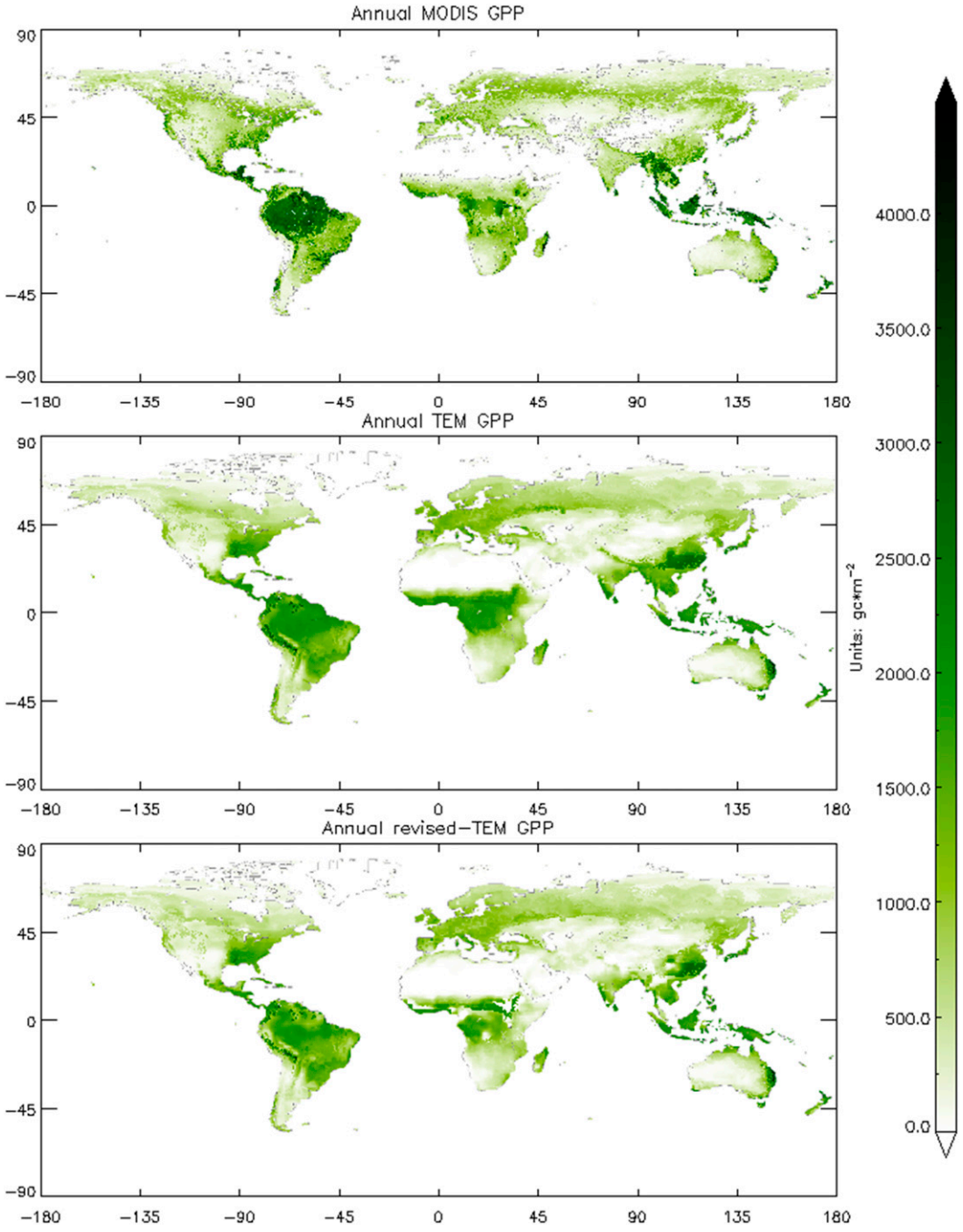

Figure 7. Annual GPP estimation comparison between MODIS GPP, TEM GPP, and revised TEM GPP for year 2010.

and polar desert and wet tundra, no changes are found within these case study regions because PDSI values are often larger than zero.

The correlation between GPP and PDSI is nonlinear (Figure 5). The direct Pearson's correlation coefficient is less than 0.5. However, some studies find the

Table 6. Comparison of total annual GPP/NPP across continents between MODIS, TEM, and revised TEM (Pg C yr^{-1}).

Continent	MODIS		TEM		Revised TEM	
	GPP	NPP	GPP	NPP	GPP	NPP
Africa	15.39	9.97	19.39	9.80	16.62	8.38
Asia	18.56	12.66	28.64	14.99	25.22	13.20
Australia	2.46	1.76	3.73	1.74	3.56	1.67
Europe	4.69	4.28	8.40	4.37	7.86	4.09
North America	10.26	7.75	13.68	7.40	12.75	6.91
South America	21.32	13.26	25.90	13.30	23.49	12.06

maximum correlation coefficient could be significant using SPI/SPEI at different temporal resolutions (Vicente-Serrano et al. 2013). The correlation would also increase when extreme drought occurs. For example, the sharp decrease in GPP in 2008 summer for temperate coniferous forests was caused by the extreme drought in 2007 winter and the following spring time (Figure 5a, yellow ellipse). Similarly, the drought explains the decrease in MODIS GPP in years 2005 and 2006 (Figure 5b, yellow ellipse). In both cases, the revised TEM was able to better capture the drought impact on GPP.

3.2. Reduction of global plant production

MODIS GPP and TEM GPP share a similar spatial pattern (Figure 6). TEM GPP tends to be overestimated compared with MODIS GPP spatially. The revised TEM GPP provides more spatial details since it considers drought impacts. When extreme droughts occur, GPP is close to 0.0 (Figure 6). The difference between two versions of TEM simulations suggests that drought impacts are significant at regional scales, especially in subtropic or tropic regions (Figure 6). Even a moderate drought in tropic or subtropic regions (e.g., Amazon tropic forests) reduces GPP significantly. Similar spatial patterns are seen in the global annual GPP. Overall, drought impacts are significant in tropical and temperate regions, and the maximum reduction exceeds 1000 g C m^{-2} yr^{-1} (Figure 6).

The drought impact accounts for 10% of the global total GPP on average from 2002 to 2010 (Figure 10). For example, the global MODIS GPP is 73.2 Pg C yr^{-1}, while previous and revised versions of TEM estimate 106.1 and 92.5 Pg C yr^{-1}, respectively (Figure 7). The average global annual GPP decreases from 106.4 to 95.7 Pg C yr^{-1} from 2002 to 2010. Extreme drought events occur in specific areas but spread worldwide, resulting in a large GPP spatial variation (Figure 6). Other studies have also shown that the drought impact on GPP across continents varies significantly (Zscheischler et al. 2014). In our study, for both Africa and Asia, the total GPP reductions from 2002 to 2010 are approximately 18%. While for Australia, the reduction is only 6%. For North America, South America, and Europe, the reduction is consistent with the global average of 10%. However, since the GPP for Asia and South America contributes over 56% to the global GPP, Asia and South America explain most of the global reduction (Table 6).

The global monthly NPP comparison shows a similar spatial pattern to global monthly GPP (Figure 7). The revised TEM estimates a consistent decrease in NPP,

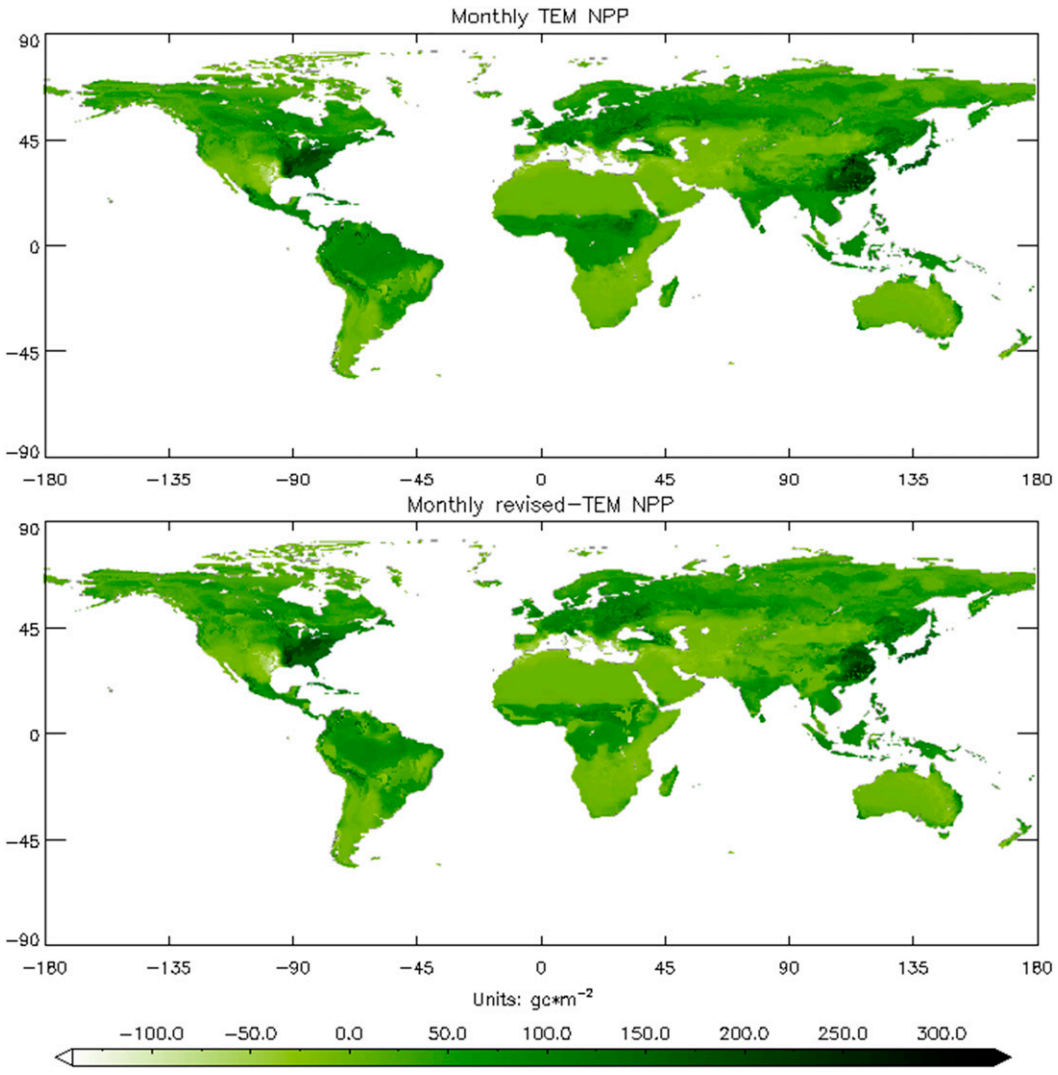

Figure 8. Monthly NPP estimation comparison for August 2010 between TEM NPP and revised TEM NPP.

though it provides more spatial variations and details in comparison with the previous TEM. The NPP differences are most significant in tropic or subtropic regions (Figure 8). The drought impacts in southern China and western Africa are captured by the revised TEM with reduction of both GPP and NPP (Figure 9).

TEM estimated annual NPP are close to MODIS NPP. However, the spatial variations of NPP show that the difference is up to 800 g C m^{-2} yr^{-1} (Figure 9). As a result of GPP decrease, NPP also decreases by 10%. The average global annual NPP decreases from 54.9 to 49.9 Pg C yr^{-1} from 2002 to 2010, while the MODIS NPP is 51.3 Pg C yr^{-1} (Figure 10). Among different continents, the NPP reduction from 2002 to 2010 for Australia (4%) and Europe (6%) is lower than that for Africa (14%) and Asia (14%). The reduction of NPP in Asia and South America dominates the global NPP reduction (Table 6).

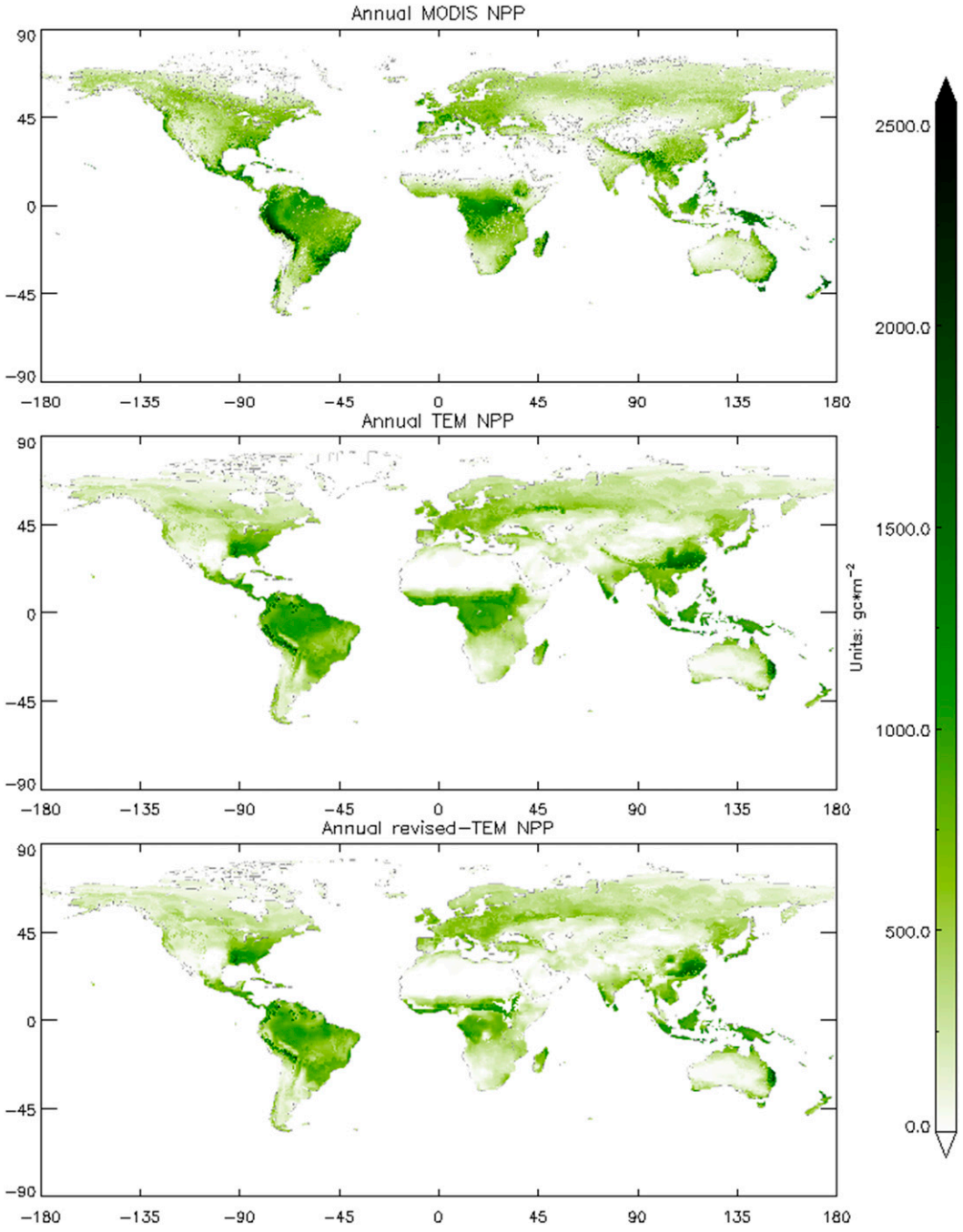

Figure 9. Annual NPP estimation between MODIS NPP, TEM NPP, and revised TEM NPP for year 2010.

3.3. Limitations

There are several limitations of our study. First, our empirical approach does not explicitly account for physiological and biochemical processes of plants' responses

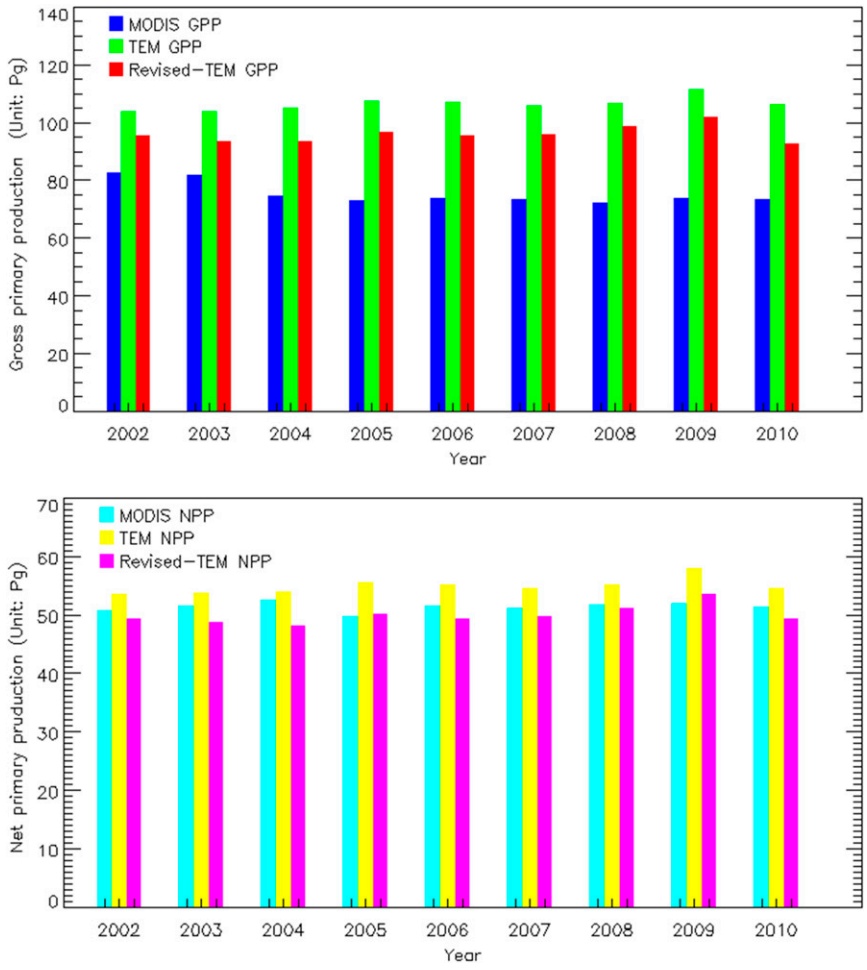

Figure 10. Global annual total GPP and NPP comparison between MODIS, TEM, and revised TEM from year 2002 to 2010. The *x* axis is the year from 2002 to 2010, and the *y* axis is the global annual total GPP and NPP estimations. Different colors represent GPP and NPP for MODIS, TEM, and revised TEM.

to droughts. Instead, the approach considers various levels of droughts through the incorporation of drought index and assumes that plants stop the photosynthesis process if the extreme drought occurs and the plant productivity decreases to 0.0 (Figure 6). Further, the empirical approach does not consider the seasonal variations. However, plants are more vulnerable to severe drought in the growing season due to greater water demand than in the nongrowing season (Welp et al. 2007). Therefore, for the same PFT, an "early drought" or "late drought," in terms of occurrence time before or after the growing season, could place different impacts on the productivity (Figure 4).

Second, the data availability remains a significant uncertainty source. First, the global GPP and NPP datasets for different PFTs are rather limited. We use the MODIS GPP product as a reference. However, it fails to capture the drought impact under certain conditions (Gebremichael and Barros 2006) or for some PFTs

(Gebremichael and Barros 2006; Heinsch et al. 2006; Turner et al. 2006). Further, MODIS GPP only covers a relatively short period from 2001 to current. Thus, using MODIS GPP to parameterize the revised TEM model might have also introduced errors to our estimates of drought impacts.

Third, PDSI may not be the most suitable drought index to account for drought impacts. As discussed earlier, there is no improvement for Arctic PFTs, such as wet tundra, because PDSI values are consistently above zero. This is because that PDSI is originally developed for semiarid climates such as Great Plains of the United States (Heim 2002; Keyantash and Dracup 2002). Further, the calculation of PDSI implies an implicit ''memory'' around 10 months (Alley 1984). Even though this memory is not the same with the time lag in our approach, it may affect our parameterization of time lags. Other drought indices (SPI/SPEI) could be alternatives to improve our approach since a few studies suggested they are more flexible in calculations (Shi et al. 2013; Vicente-Serrano et al. 2013). In addition, the determination of lower and upper bounds during parameterization has considered the PDSI classification (Table 1). However, these criteria need to be further examined since plants may still be able to maintain photosynthesis under extreme droughts (Reddy et al. 2004).

4. Conclusions

This study develops an empirical approach to estimate the drought impact on ecosystem productivity. MODIS GPP data are used for the model parameterization and verification. This approach improves GPP and NPP estimates using an ecosystem model under various drought conditions. Our analysis indicates that the global GPP decreased from 106.4 to 95.7 $\mathrm{Pg\,C\,yr^{-1}}$, and global NPP decreased from 54.9 to 49.9 $\mathrm{Pg\,C\,yr^{-1}}$ due to droughts from 2002 to 2010. Our analysis suggests that, to improve the quantification of drought impacts, physiological and biochemical processes shall be incorporated into ecosystem modeling. In addition, more in situ observation data of droughts and carbon fluxes for different plant functional types are needed.

Acknowledgments. This research was funded by the NSF Project (Grant IIS-1028291; A Paradigm Shift in Ecosystem and Environmental Modeling: An Integrated Stochastic, Deterministic, and Machine Learning Approach). We thank Yujie He and Xudong Zhu for assistance with model parameterization.

References

Alley, W. M., 1984: The Palmer drought severity index: Limitations and assumptions. *J. Climate Appl. Meteor.*, **23**, 1100–1109, doi:10.1175/1520-0450(1984)023<1100:TPDSIL>2.0.CO;2.

Barber, V. A., G. P. Juday, and B. P. Finney, 2000: Reduced growth of Alaskan white spruce in the twentieth century from temperature-induced drought stress. *Nature*, **405**, 668–673, doi:10.1038/35015049.

Brock, M. T., and C. Galen, 2005: Drought tolerance in the alpine dandelion, *Taraxacum ceratophorum* (Asteraceae), its exotic congener *T. officinale*, and interspecific hybrids under natural and experimental conditions. *Amer. J. Bot.*, **92**, 1311–1321, doi:10.3732/ajb.92.8.1311.

Chaves, M. M., J. P. Maroco, and J. S. Pereira, 2003: Understanding plant responses to drought-from genes to the whole plant. *Funct. Plant Biol.*, **30**, 239–264, doi:10.1071/FP02076.

Chen, G., and Coauthors, 2012: Drought in the southern United States over the 20th century: Variability and its impacts on terrestrial ecosystem productivity and carbon storage. *Climatic Change*, **114**, 379–397, doi:10.1007/s10584-012-0410-z.

Chen, M., Q. Zhuang, D. R. Cook, R. Coulter, M. Pekour, R. L. Scott, J. W. Munger, and K. Bible, 2011: Quantification of terrestrial ecosystem carbon dynamics in the conterminous United States combining a process-based biogeochemical model and MODIS and AmeriFlux data. *Biogeosci. Discuss.*, **8**, 2665–2688, doi:10.5194/bg-8-2665-2011.

Ciais, P., and Coauthors, 2005: Europe-wide reduction in primary productivity caused by the heat and drought in 2003. *Nature*, **437**, 529–533, doi:10.1038/nature03972.

Craine, J. M., T. W. Ocheltree, J. B. Nippert, E. G. Towne, A. M. Skibbe, S. W. Kembel, and J. E. Fargione, 2012: Global diversity of drought tolerance and grassland climate-change resilience. *Nat. Climate Change*, **3**, 63–67, doi:10.1038/nclimate1634.

Dai, A., 2011: Drought under global warming: A review. *Wiley Interdiscip. Rev.: Climate Change*, **2**, 45–65, doi:10.1002/wcc.81.

Duan, Q., S. Sorooshian, and V. K. Gupta, 1994: Optimal use of the SCE-UA global optimization method for calibrating watershed models. *J. Hydrol.*, **158**, 265–284, doi:10.1016/0022-1694(94)90057-4.

Eilmann, B., R. Zweifel, N. Buchmann, E. G. Pannatier, and A. Rigling, 2011: Drought alters timing, quantity, and quality of wood formation in Scots pine. *J. Exp. Bot.*, **62**, 2763–2771, doi:10.1093/jxb/erq443.

Engelbrecht, B. M., L. S. Comita, R. Condit, T. A. Kursar, M. T. Tyree, B. L. Turner, and S. P. Hubbell, 2007: Drought sensitivity shapes species distribution patterns in tropical forests. *Nature*, **447**, 80–82, doi:10.1038/nature05747.

Gebremichael, M., and A. P. Barros, 2006: Evaluation of MODIS gross primary productivity (GPP) in tropical monsoon regions. *Remote Sens. Environ.*, **100**, 150–166, doi:10.1016/j.rse.2005.10.009.

Guttman, N. B., 1998: Comparing the Palmer drought index and the standardized precipitation index. *J. Amer. Water Resour. Assoc.*, **34**, 113–121, doi:10.1111/j.1752-1688.1998.tb05964.x.

Hashimoto, H., and Coauthors, 2012: Exploring simple algorithms for estimating gross primary production in forested areas from satellite data. *Remote Sens.*, **4**, 303–326, doi:10.3390/rs4010303.

Heim, R. R., Jr., 2002: A review of twentieth-century drought indices used in the United States. *Bull. Amer. Meteor. Soc.*, **83**, 1149–1165, doi:10.1175/1520-0477(2002)083<1149:AROTDI>2.3.CO;2.

Heinsch, F. A., and Coauthors, 2003: User's guide GPP and NPP (MOD17A2/A3) products NASA MODIS land algorithm. MOD17 User's Guide, 57 pp.

——, and Coauthors, 2006: Evaluation of remote sensing based terrestrial productivity from MODIS using regional tower eddy flux network observations. *IEEE Trans. Geosci. Remote Sens.*, **44**, 1908–1925, doi:10.1109/TGRS.2005.853936.

Huete, A., K. Didan, T. Miura, E. P. Rodriguez, X. Gao, and L. G. Ferreira, 2002: Overview of the radiometric and biophysical performance of the MODIS vegetation indices. *Remote Sens. Environ.*, **83**, 195–213, doi:10.1016/S0034-4257(02)00096-2.

IPCC, 2013: *Climate Change 2013: The Physical Science Basis*. Cambridge University Press, 1535 pp.

Keyantash, J., and J. A. Dracup, 2002: The quantification of drought: An evaluation of drought indices. *Bull. Amer. Meteor. Soc.*, **83**, 1167–1180, doi:10.1175/1520-0477(2002)083<1191:TQODAE>2.3.CO;2.

Kumagai, T., and A. Porporato, 2012: Drought-induced mortality of a Bornean tropical rain forest amplified by climate change. *J. Geophys. Res.*, **117**, G02032, doi:10.1029/2011JG001835.

Lévesque, M., M. Saurer, R. Siegwolf, B. Eilmann, P. Brang, H. Bugmann, and A. Rigling, 2013: Drought response of five conifer species under contrasting water availability suggests high

vulnerability of Norway spruce and European larch. *Global Change Biol.*, **19**, 3184–3199, doi:10.1111/gcb.12268.

McDowell, N. G., and Coauthors, 2008: Mechanisms of plant survival and mortality during drought: Why do some plants survive while others succumb to drought? *New Phytol.*, **178**, 719–739, doi:10.1111/j.1469-8137.2008.02436.x.

McKee, T. B., N. J. Doesken, and J. Kleist, 1993: The relationship of drought frequency and duration to time scales. *Proc. Eighth Conf. on Applied Climatology*, Boston, MA, Amer. Meteor. Soc., 179–183.

Mu, Q., M. Zhao, J. S. Kimball, N. G. McDowell, and S. W. Running, 2013: A remotely sensed global terrestrial drought severity index. *Bull. Amer. Meteor. Soc.*, **94**, 83–98, doi:10.1175/BAMS-D-11-00213.1.

NOAA National Centers for Environmental Information, 2010: State of the climate: Global hazards for February 2010. Accessed 15 June 2013. [Available online at http://www.ncdc.noaa.gov/sotc/hazards/201002.]

Palmer, W. C., 1965: Meteorological drought. U.S. Department of Commerce Research Paper 45, 65 pp.

Peng, C., and Coauthors, 2011: A drought-induced pervasive increase in tree mortality across Canada's boreal forests. *Nat. Climate Change*, **1**, 467–471, doi:10.1038/nclimate1293.

Phillips, O. L., and Coauthors, 2009: Drought sensitivity of the Amazon rainforest. *Science*, **323**, 1344–1347, doi:10.1126/science.1164033.

Planton, S., Ed., 2013: Annex III: Glossary. *Climate Change 2013: The Physical Science Basis*, T. F. Stocker et al., Eds., Cambridge University Press, 1447–1466.

Rajan, N., S. J. Maas, and S. Cui, 2013: Extreme drought effects on carbon dynamics of a semiarid pasture. *Agron. J.*, **105**, 1749–1760, doi:10.2134/agronj2013.0112.

Reddy, A. R., K. V. Chaitanya, and M. Vivekanandan, 2004: Drought-induced responses of photosynthesis and antioxidant metabolism in higher plants. *J. Plant Physiol.*, **161**, 1189–1202, doi:10.1016/j.jplph.2004.01.013.

Reichstein, M., and Coauthors, 2013: Climate extremes and the carbon cycle. *Nature*, **500**, 287–295, doi:10.1038/nature12350.

Reyer, C. P., and Coauthors, 2013: A plant's perspective of extremes: Terrestrial plant responses to changing climatic variability. *Global Change Biol.*, **19**, 75–89, doi:10.1111/gcb.12023.

Rossini, M., and Coauthors, 2012: Remote sensing-based estimation of gross primary production in a subalpine grassland. *Biogeosciences*, **9**, 2565–2584, doi:10.5194/bg-9-2565-2012.

Rouault, M., and Y. Richard, 2003: Intensity and spatial extension of drought in South Africa at different time scales. *Water S.A.*, **29**, 489–500, doi:10.4314/wsa.v29i4.5057.

Sala, A., F. Piper, and G. Hoch, 2010: Physiological mechanisms of drought-induced tree mortality are far from being resolved. *New Phytol.*, **186**, 274–281, doi:10.1111/j.1469-8137.2009.03167.x.

Shi, Z., and Coauthors, 2013: Differential effects of extreme drought on production and respiration: Synthesis and modeling analysis. *Biogeosci. Discuss.*, **11**, 621–633, doi:10.5194/bg-11-621-2014.

Sitch, S., and Coauthors, 2003: Evaluation of ecosystem dynamics, plant geography and terrestrial carbon cycling in the LPJ dynamic global vegetation model. *Global Change Biol.*, **9**, 161–185, doi:10.1046/j.1365-2486.2003.00569.x.

——, and Coauthors, 2008: Evaluation of the terrestrial carbon cycle, future plant geography and climate-carbon cycle feedbacks using five dynamic global vegetation models (DGVMs). *Global Change Biol.*, **14**, 2015–2039, doi:10.1111/j.1365-2486.2008.01626.x.

Tarantola, A., 2005: *Inverse Problem Theory and Methods for Model Parameter Estimation*. Siam, 339 pp.

Thiemann, M., M. Trosset, H. Gupta, and S. Sorooshian, 2001: Bayesian recursive parameter estimation for hydrologic models. *Water Resour. Res.*, **37**, 2521–2535, doi:10.1029/2000WR900405.

Turner, D. P., and Coauthors, 2006: Evaluation of MODIS NPP and GPP products across multiple biomes. *Remote Sens. Environ.*, **102**, 282–292, doi:10.1016/j.rse.2006.02.017.

Vicente-Serrano, S. M., S. Beguería, and J. I. López-Moreno, 2010: A multiscalar drought index sensitive to global warming: The standardized precipitation evapotranspiration index. *J. Climate*, **23**, 1696–1718, doi:10.1175/2009JCLI2909.1.

——, and Coauthors, 2012: Drought impacts on vegetation activity, growth and primary production in humid and arid ecosystems. Accessed 15 June 2014. [Available online at http://digital.csic.es/bitstream/10261/62153/1/BegueriaS_Drought_ComCongSal-AEC_2012.pdf.]

——, and Coauthors, 2013: Response of vegetation to drought time-scales across global land biomes. *Proc. Natl. Acad. Sci. USA*, **110**, 52–57, doi:10.1073/pnas.1207068110.

——, J. J. Camarero, J. Zabalza, G. Sangüesa-Barreda, J. I. López-Moreno, and C. Tague, 2015: Evapotranspiration deficit controls net primary production and growth of silver fir: Implications for circum-Mediterranean forests under forecasted warmer and drier conditions. *Agric. For. Meteor.*, **206**, 45–54, doi:10.1016/j.agrformet.2015.02.017.

Wang, J., K. Price, and P. Rich, 2001: Spatial patterns of NDVI in response to precipitation and temperature in the central Great Plains. *Int. J. Remote Sens.*, **22**, 3827–3844, doi:10.1080/01431160010007033.

Wells, N., S. Goddard, and M. J. Hayes, 2004: A self-calibrating Palmer drought severity index. *J. Climate*, **17**, 2335–2351, doi:10.1175/1520-0442(2004)017<2335:ASPDSI>2.0.CO;2.

Welp, L., J. Randerson, and H. Liu, 2007: The sensitivity of carbon fluxes to spring warming and summer drought depends on plant functional type in boreal forest ecosystems. *Agric. For. Meteor.*, **147**, 172–185, doi:10.1016/j.agrformet.2007.07.010.

Zhao, M., and S. W. Running, 2010: Drought-induced reduction in global terrestrial net primary production from 2000 through 2009. *Science*, **329**, 940–943, doi:10.1126/science.1192666.

Zhuang, Q., and Coauthors, 2003: Carbon cycling in extratropical terrestrial ecosystems of the Northern Hemisphere during the 20th century: A modeling analysis of the influences of soil thermal dynamics. *Tellus*, **55B**, 751–776, doi:10.1034/j.1600-0889.2003.00060.x.

——, J. He, Y. Lu, L. Ji, J. Xiao, and T. Luo, 2010: Carbon dynamics of terrestrial ecosystems on the Tibetan Plateau during the 20th century: An analysis with a process-based biogeochemical model. *Global Ecol. Biogeogr.*, **19**, 649–662, doi:10.1111/j.1466-8238.2010.00559.x.

Zscheischler, J., M. Reichstein, S. Harmeling, A. Rammig, E. Tomelleri, and M. D. Mahecha, 2014: Extreme events in gross primary production: A characterization across continents. *Biogeosciences*, **11**, 2909–2924, doi:10.5194/bg-11-2909-2014.

Earth Interactions is published jointly by the American Meteorological Society, the American Geophysical Union, and the Association of American Geographers. Permission to use figures, tables, and *brief* excerpts from this journal in scientific and educational works is hereby granted provided that the source is acknowledged. Any use of material in this journal that is determined to be "fair use" under Section 107 or that satisfies the conditions specified in Section 108 of the U.S. Copyright Law (17 USC, as revised by P.IL. 94-553) does not require the publishers' permission. For permission for any other from of copying, contact one of the copublishing societies.